Yokohama Publishers
ISSN 1349-8169 ONLINE JOURNAL

Pacific Journal of Optimization
Vol. 9, No. 3, pp. 427–442, July 2013

AN EFFICIENT COMPUTATIONAL APPROACH TO MINIMUM-FUEL LOW-THRUST NON-COPLANAR ORBIT TRANSFER*

Da-Ke Gu† and Ling-Fang Sun

Abstract: In this paper, the optimal trajectories for non-coplanar circular-to-circular orbit transfer with a constant thrust of which the direction is controllable are solved. To circumvent the complexity of the purely numerical methods, an efficient computational method is proposed. By the control parametrization technique in conjunction with a time scaling transform, the optimal trajectories of non-coplanar orbit transfer problem is approximated by a sequence of optimal parameter selection problems. Each of these approximate optimization problems can be viewed as a nonlinear mathematical programming problem, and we develop a numerical scheme for computing the relevant gradients. On this basis, each approximate problem can be solved using existing gradient-based optimization techniques. Numerical results are presented for illustration.

Key words: *low-thrust orbit transfer, optimal control, control parametrization technique, time scaling transform*

Mathematics Subject Classification: *49N90, 90C90, 93C95*

1 Introduction

The problem of obtaining optimal orbit transfers using low-thrust propulsion has been investigated in great detail. Low-thrust high-specific-impulse solar electric propulsion systems offer more payload than those propelled by conventional chemical propulsion. However, Earth-orbit transfers using low-thrust propulsion usually result in prolonged flight time. Due to this characteristic, optimizing low-thrust transfer trajectories has been considered a challenging optimal control problem in the past decades.

Low-thrust trajectory optimization techniques fall into two categories: indirect methods and direct methods. Indirect methods solve the optimal control problem by obtaining the solution to the corresponding two-point boundary value problem (2PBVP), which results from the calculus of variations. A drawback to indirect methods is that the 2PBVP is usually very sensitive and extremely difficult to solve unless a good initial guess for the unknown initial costate variables is available. An advantage of indirect methods is that if the solution to the 2PBVP is obtained, then the resulting trajectory is (in most cases) optimal. In contrast, direct methods solve the optimal control problem by adjusting the

*Research Supported by National Natural Science Foundation of China (No. 61074111) , Educational Commission of Jilin Province, China (No. 2013122), and Research Fund for Doctor of Northeast Dianli University of China (No. BSJXM-201105).

†Corresponding author

ISSN 1348-9151

control variables at each iteration in an attempt to continually reduce the performance index. One advantage of direct methods is that it is usually easier to produce a good initial control guess, which typically results in a more robust optimization method. A drawback to direct methods is that convergence to the solution may be slower compared to indirect methods. Betts [3] used the direct transcription method to solve a transfer from Earth to Mars including a swing by of the planets Venus, recognizing its effectiveness in solving trajectory optimization problems. Also in 1994, using accumulated velocity change to replace the time-of-flight and to account for propellant mass loss, Alfano and Thorne [1] developed some simple graphical/anlytical tools to determine the minimum elapsed time and associated fuel of a constant-thrust vehicle for circle-to-circle coplanar transfers. Scheel and Conway [13] developed a parallel Runge-Kutta method for solving low-thrust orbit transfers. Tang and Conway [14] used the method of collocation with nonlinear programming to determine the minimum-time, low-thrust interplanetary transfer trajectories. Kluever and Pierson [11] used a "hybrid" direct/indirect method to solve the minimum-fuel Earth-Moon transfer to a polar lunar orbit for a low-thrust spacecraft. Herman and Conway [6] solved the low-thrust orbit transfer using collocation based on high-order Gauss-Lobatto quadrature rules. Thorne and Hall [15] used the shooting method to solve the minimum time orbit transfer problem with continuous thrust. Kluever [10] developed a direct optimization method and utilized it to compute a wide range of optimal low-thrust interplanetary trajectories. Herman and Conway [7] used the method of collocation with nonlinear programming to determine the minimum-fuel, low-thrust, Earth-Moon orbit transfer. Herman and Spencer [8] used a trajectory optimization technique based upon higher-order collocation to solve optimal, low-thrust, Earth orbit transfer problems. Chen and Sheu [5] used parametric method and second-order gradient method to solve minimum fuel low-thrust coplanar orbit transfer.

This paper presents a new computational method for obtaining minimum-fuel low-thrust non-coplanar orbit transfer. Our method is based on control parametrization technique and time scaling transform. We employ a piecewise constant approximation of control to derive a class of approximate optimization problems. To solve these approximate problems using conventional optimization algorithms, the gradients of the objective function with respect to the decision parameters are derived. Finally, we use our algorithm to solve the minimum-fuel low-thrust non-coplanar orbit transfer problem.

2 Problem Formulation

2.1 Dynamics of Motion

In this subsection, the geocentric inertial coordinate system is used to describe the motion of the spacecraft. The origin of the geocentric system is at the Earth's center, and the fundamental plane of this system is the original orbital plane which is defined as the x-y plane. The positive x axis points in the direction of initial position vector, and the y axis is 90° in the direction of motion from the x axis. The z axis is thus orthogonal to the original orbital plane. The unit vectors which lie along the x, y, and z axes are $\boldsymbol{i}$, $\boldsymbol{j}$ and $\boldsymbol{k}$, respectively. For convenience of derivation, a moving coordinate system is attached onto the spacecraft. Let $\boldsymbol{e}_r$ be the unit vector in the position vector $\boldsymbol{r}$ direction, $\boldsymbol{e}_\theta$ and $\boldsymbol{e}_\phi$ the unit vectors in the direction of increasing the range angle θ and the out-of-plane angle ϕ, respectively, as shown in Figure 1. The direction of thrust, as shown in Figure 2, where φ and τ both are in-plane and the out-of-plane thrust control angles of the spacecraft, then the equations of motion for the spacecraft can be derived as follows [4]:

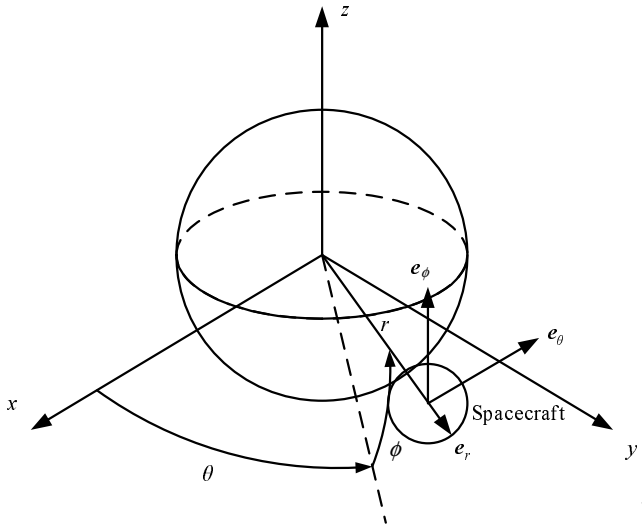

Figure 1: Coordinate system

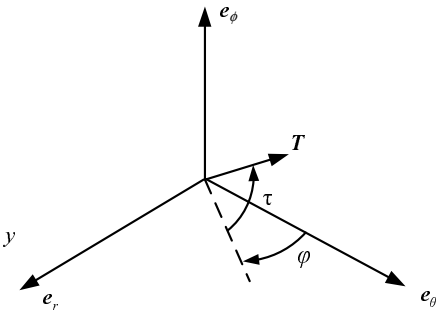

Figure 2: Direction of thrust

$$\begin{cases} \dot{r} = u \\ \dot{\theta} = \dfrac{v}{r\cos\phi} \\ \dot{\phi} = \dfrac{w}{r} \\ \dot{u} = \dfrac{v^2}{r} + \dfrac{w^2}{r} - \dfrac{\mu}{r^2} + \dfrac{T\sin\varphi\cos\tau}{m} \\ \dot{v} = -\dfrac{uv}{r} + \dfrac{vw\tan\phi}{r} + \dfrac{T\cos\varphi\cos\tau}{m} \\ \dot{w} = -\dfrac{uw}{r} - \dfrac{v^2\tan\phi}{r} + \dfrac{T\sin\tau}{m} \\ \dot{m} = -\dfrac{T}{g_0 i_{sp}} \end{cases} \tag{2.1}$$

where r is the radial distance from the center of Earth to the spacecraft, u, v and w the speed component, respectively, m the mass of the spacecraft. In the above equations, the thrust T is assumed to be constant, $\varphi\,(-\pi < \varphi \le \pi)$ and $\tau\,(-\pi/2 \le \tau \le \pi/2)$ are the control variables. Also, μ is the gravitational parameter of the Earth, i_{sp} the specific impulse, and g_0 the gravitational acceleration on the Earth's surface.

2.2 Terminal Conditions

The classical orbital elements i and Ω are used to specify the circular target orbit plane. As shown in Figure 3, i is the inclination angle between the original and the target orbital planes and Ω is the longitude of intersection of the original and the target orbital planes, counted in the original orbital plane from the x axis. If the radius of the circular target orbit as r_f, then the final distance from the center of the Earth to the spacecraft must be

$$r(t_f) = r_f \tag{2.2a}$$

Also, for circular target orbit, the radial component of the velocity must vanish, i.e.,

$$u(t_f) = 0 \tag{2.2b}$$

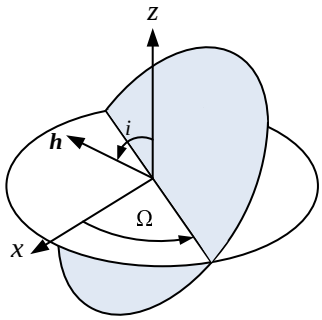

Figure 3: Non-coplanar orbit transfer: circular target orbit

and the magnitude of the velocity must be equal to $\sqrt{\mu/r_f}$, or,

$$v^2(t_f) + w^2(t_f) = \frac{\mu}{r_f} \tag{2.2c}$$

In addition to the above three conditions, at the final time t_f, the transfer orbit must match the specified inclination and longitude. The angular momentum for a circular orbit is

$$\boldsymbol{h} = \boldsymbol{r} \times \boldsymbol{V} = r\boldsymbol{e}_r \times (v\boldsymbol{e}_\theta + w\boldsymbol{e}_\phi) = -rw\boldsymbol{e}_\theta + rv\boldsymbol{e}_\phi \tag{2.3}$$

Accordingly, the magnitude of $\boldsymbol{h}$ is

$$h = \sqrt{\boldsymbol{h} \cdot \boldsymbol{h}} = r\sqrt{v^2 + w^2} = r\sqrt{\frac{\mu}{r}} = \sqrt{r\mu} \tag{2.4}$$

and the unit vector in $\boldsymbol{h}$ direction is

$$\boldsymbol{e}_h \triangleq \frac{\boldsymbol{h}}{h} = \sqrt{\frac{r}{\mu}}(-w\boldsymbol{e}_\theta + v\boldsymbol{e}_\phi) \tag{2.5}$$

According to the definition of i and Ω,

$$\boldsymbol{k} \cdot \boldsymbol{e}_h = \cos i \tag{2.6}$$

$$\boldsymbol{k} \times \boldsymbol{e}_h = \sin i\boldsymbol{e}_n = \sin i(\cos\Omega\boldsymbol{i} + \sin\Omega\boldsymbol{j}) \tag{2.7}$$

where $\boldsymbol{e}_n$ is the unit vector in the ascending node direction. Substituting the following equation

$$\boldsymbol{k} = \sin\phi\boldsymbol{e}_r + \cos\phi\boldsymbol{e}_\theta \tag{2.8}$$

and (2.5) into the following (2.6) leads to

$$\sqrt{\frac{r}{\mu}}v\cos\phi = \cos i \quad \text{or} \quad v\cos\phi = \sqrt{\frac{\mu}{r}}\cos i \tag{2.9}$$

In (2.5), $\boldsymbol{e}_h$ can also be represented with the inertial coordinate system

$$\boldsymbol{e}_h = \sqrt{\frac{r}{\mu}}\left[(-v\sin\phi\cos\theta + w\sin\theta)\boldsymbol{i} + (-v\sin\phi\sin\theta - w\cos\theta)\boldsymbol{j} + (v\cos\phi)\boldsymbol{k}\right] \tag{2.10}$$

which is then substituted into (2.6) and (2.7) to obtain

$$\sqrt{\frac{r}{\mu}} v \cos\phi = \cos i \tag{2.11a}$$

and

$$\sqrt{\frac{r}{\mu}} \left[(v \sin\phi \sin\theta + w \cos\theta)\boldsymbol{i} + (-v \sin\phi \cos\theta + w \sin\theta)\boldsymbol{j} \right] = \sin i (\cos\Omega \boldsymbol{i} + \sin\Omega \boldsymbol{j}) \tag{2.11b}$$

respectively. Compare the coefficients of $\boldsymbol{i}$ and $\boldsymbol{j}$ on both sides of the last equation gives

$$\sqrt{\frac{r}{\mu}} (v \sin\phi \sin\theta + w \cos\theta) = \sin i \cos\Omega \tag{2.11c}$$

$$\sqrt{\frac{r}{\mu}} (-v \sin\phi \cos\theta + w \sin\theta) = \sin i \sin\Omega \tag{2.11d}$$

It is obvious from (2.11), the three additional final conditions which must be satisfied are

$$v(t_f) \cos\phi(t_f) = \sqrt{\frac{\mu}{r_f}} \cos i \tag{2.12a}$$

$$v(t_f) \sin\phi(t_f) \sin\theta(t_f) + w(t_f) \cos\theta(t_f) = \sqrt{\frac{\mu}{r_f}} \sin i \cos\Omega \tag{2.12b}$$

$$-v(t_f) \sin\phi(t_f) \cos\theta(t_f) + w(t_f) \sin\theta(t_f) = \sqrt{\frac{\mu}{r_f}} \sin i \sin\Omega \tag{2.12c}$$

In summary, the terminal constraint conditions for the non-coplanar orbit transfer to circular target orbit are (2.2a), (2.2b) and (2.12).

2.3 Non-coplanar Orbit Transfer

It is known that if the fuel is minimized, it is equivalent to that the final mass is maximized. Therefore, the cost function is defined as follows:

$$J = -m(t_f) \tag{2.13}$$

For (2.1), we introduce two new state equations

$$\dot{\varphi} = \alpha \tag{2.14}$$

$$\dot{\tau} = \beta \tag{2.15}$$

Let

$$\begin{aligned} \boldsymbol{x} &= [r,\ \theta,\ \phi,\ u,\ v,\ w,\ m,\ \varphi,\ \tau]^{\mathrm{T}} \\ &= [x_1,\ x_2,\ x_3,\ x_4,\ x_5,\ x_6,\ x_7,\ x_8,\ x_9]^{\mathrm{T}} \end{aligned} \tag{2.16}$$

and

$$\boldsymbol{u} = [u_1,\ u_2]^{\mathrm{T}} = [\alpha,\ \beta]^{\mathrm{T}} \tag{2.17}$$

The original system dynamics (2.1) can be rewritten in the form of the non-linear system given below

$$\dot{\boldsymbol{x}} = \boldsymbol{f}(\boldsymbol{x}(t)) + \boldsymbol{B}\boldsymbol{u}(t) \tag{2.18}$$

and

$$\boldsymbol{f}(\boldsymbol{x}) = \begin{bmatrix} u \\ \dfrac{v}{r\cos\phi} \\ \dfrac{w}{r} \\ \dfrac{v^2}{r} + \dfrac{w^2}{r} - \dfrac{\mu}{r^2} + \dfrac{T\sin\varphi\cos\tau}{m} \\ -\dfrac{uv}{r} + \dfrac{vw\tan\phi}{r} + \dfrac{T\cos\varphi\cos\tau}{m} \\ -\dfrac{uw}{r} - \dfrac{v^2\tan\phi}{r} + \dfrac{T\sin\tau}{m} \\ -\dfrac{T}{g_0 i_{sp}} \\ 0 \\ 0 \end{bmatrix} \tag{2.19}$$

$$\boldsymbol{B} = \begin{bmatrix} 0 & 0 & 0 & 0 & 0 & 0 & 0 & 1 & 0 \\ 0 & 0 & 0 & 0 & 0 & 0 & 0 & 0 & 1 \end{bmatrix}^{\mathrm{T}} \tag{2.20}$$

and subject to the following inequality constraints

$$-\pi < x_8(t) \le \pi, \ -\frac{\pi}{2} \le x_9(t) \le \frac{\pi}{2}, \ \forall t \in [0, t_f] \tag{2.21}$$

There are no bound on the control variable $\boldsymbol{u}$. Let $\mathcal{U}$ be the set of all such controls $\boldsymbol{u}$.

According to (2.2a), (2.2b) and (2.12), the terminal conditions are listed as

$$\begin{cases} x_1(t_f) = r_f \\ x_4(t_f) = 0 \\ x_5(t_f)\cos(x_3(t_f)) = \sqrt{\dfrac{\mu}{r_f}}\cos i \\ x_5(t_f)\sin(x_3(t_f))\sin(x_2(t_f)) + x_6(t_f)\cos(x_2(t_f)) = \sqrt{\dfrac{\mu}{r_f}}\sin i\cos\Omega \\ -x_5(t_f)\sin(x_3(t_f))\cos(x_2(t_f)) + x_6(t_f)\sin(x_2(t_f)) = \sqrt{\dfrac{\mu}{r_f}}\sin i\sin\Omega \end{cases} \tag{2.22}$$

We may now state our minimum-fuel low-thrust non-coplanar orbit transfer problem as follows.

Problem 2.1 (P)**.** Given the dynamical system (2.18), find a control $\boldsymbol{u} \in \mathcal{U}$ such that the cost function (2.13) is minimized subject to the state inequality constraints (2.21) and the terminal state constraints (2.22).

3 Computation Method

To solve Problem (P), we shall apply the control parametrization scheme [16] together with a time scaling transform [12, 17]. The time horizon $[0, t_f]$ is partitioned by a monotonically increasing sequence $\{t_0, t_1, \cdots, t_p\}$. Then, the control is approximated by a piecewise constant function

$$u_1^p(t) = \sum_{k=1}^{p} \sigma_1^k \chi_{[t_{k-1}, t_k)}(t) \tag{3.1a}$$

$$u_2^p(t) = \sum_{k=1}^{p} \sigma_2^k \chi_{[t_{k-1},t_k)}(t) \tag{3.1b}$$

where $t_{k-1} \le t_k,\ k = 1, \ldots, p$, with $t_0 = 0$ and $t_p = t_f$, and

$$\chi_I(t) = \begin{cases} 1 & t \in I \\ 0 & \text{otherwise} \end{cases} \tag{3.2}$$

For each $j = 1, 2$, and $k = 1, 2, \ldots, p$, σ_j^k is a constant control parameter. Let $\boldsymbol{\sigma}^k = \left[\sigma_j^1, \cdots, \sigma_j^p\right]^{\mathrm{T}}$, and let $\boldsymbol{\sigma} = \left[(\boldsymbol{\sigma}^1)^{\mathrm{T}},\ \cdots,\ (\boldsymbol{\sigma}^p)^{\mathrm{T}}\right]^{\mathrm{T}}$ Define $\boldsymbol{u}^p = [u_1^p,\ u_2^p]^{\mathrm{T}}$. As $\boldsymbol{u}^p \in \mathcal{U}$, it is clear that $\boldsymbol{\sigma}$ satisfies no boundedness. Let Ξ denote the set containing all such $\boldsymbol{\sigma}$.

The switching times $t_k, 1 \le k \le p-1$, are regarded as additional decision variables. We shall employ the time scaling transform to map these switching times into a set of fixed time points $k/p, k = 1, \ldots, p-1$, on a new time horizon $[0, 1]$. This is easily achieved by the differential equation

$$\frac{\mathrm{d}t(s)}{\mathrm{d}s} = \vartheta^p(s),\ s \in [0, 1] \tag{3.3}$$

with initial condition

$$t(0) = 0 \tag{3.4}$$

where

$$\vartheta^p(s) = \sum_{k=1}^{p} \gamma_k \chi_{\left[\frac{k-1}{p}, \frac{k}{p}\right)}(s) \tag{3.5}$$

Here $\gamma_k \ge 0, k = 1, \ldots, p$, and

$$\sum_{k=1}^{p} \frac{\gamma_k}{p} = t_f \tag{3.6}$$

Let $\boldsymbol{\gamma} = [\gamma_1, \ldots, \gamma_p]^{\mathrm{T}}$ and let Υ be the set containing all such $\boldsymbol{\gamma}$.

Integrating (3.3) with initial condition (3.4), it is easy to see that

$$t(s) = \sum_{k=1}^{q-1} \frac{\gamma_k}{p} + \frac{\gamma_q}{p}(ps - q + 1),\ q = 1, \ldots, p,\ s \in \left[\frac{q-1}{p}, \frac{q}{p}\right). \tag{3.7}$$

Clearly, $t(1) = t_f$. The approximate control given by (3.1) in the new time horizon $[0, 1]$ becomes

$$\hat{\boldsymbol{u}}^p(s) = \boldsymbol{u}^p(t(s)) = \sum_{k=1}^{p} \boldsymbol{\sigma}^k \chi_{\left[\frac{k-1}{p}, \frac{k}{p}\right)}(s) \tag{3.8}$$

which has fixed switching times at $s = 1/p, \ldots, (p-1)/p$. Now, by using the time scaling transform (3.3)–(3.6), the dynamic system (2.18) and (3.3) are transformed into

$$\frac{\mathrm{d}\hat{\boldsymbol{x}}(s)}{\mathrm{d}s} = \hat{\boldsymbol{f}}(s, \hat{\boldsymbol{x}}(s), \boldsymbol{\sigma}, \boldsymbol{\gamma}) = \begin{bmatrix} \vartheta^p(s)\, \boldsymbol{f}(\boldsymbol{x}(t(s)), \hat{\boldsymbol{u}}^p(s)) \\ \vartheta^p(s) \end{bmatrix} \tag{3.9}$$

where $\hat{\boldsymbol{x}} = [\boldsymbol{x}(t(s)), t(s)]^{\mathrm{T}}$.

The cost function (2.13) yields

$$\hat{J} = -\hat{m}(1) \tag{3.10}$$

From (2.21) have

$$-\pi < \hat{x}_8(s) \le \pi,\ -\frac{\pi}{2} \le \hat{x}_9(s) \le \frac{\pi}{2},\ \forall s \in [0, 1] \tag{3.11}$$

and the terminal state constraints (2.22) transform into

$$\hat{\boldsymbol{g}} = \begin{bmatrix} \hat{x}_1(1) - r_f \\ \hat{x}_4(1) \\ \hat{x}_5(1)\cos(\hat{x}_3(1)) - \sqrt{\frac{\mu}{r_f}}\cos i \\ \hat{x}_5(1)\sin(\hat{x}_3(1))\sin(\hat{x}_2(1)) + \hat{x}_6(1)\cos(\hat{x}_2(1)) - \sqrt{\frac{\mu}{r_f}}\sin i\cos\Omega \\ -\hat{x}_5(1)\sin(\hat{x}_3(1))\cos(\hat{x}_2(1)) + \hat{x}_6(1)\sin(\hat{x}_2(1)) - \sqrt{\frac{\mu}{r_f}}\sin i\sin\Omega \\ t(1) - t_f \end{bmatrix} = \mathbf{0} \quad (3.12)$$

The original minimum-fuel low-thrust non-coplanar orbit transfer Problem (P) is now approximated by a sequence of optimal parameter selection problems depending on p, the number of the partition points of the time horizon $[0, t_f]$, given below.

Problem 3.1 ($\hat{\text{P}}$)**.** Given system (3.9) on the time interval $s \in [0,1]$, find a control parameter vector $\boldsymbol{\sigma} \in \Xi$ and a switching time vector $\boldsymbol{\gamma} \in \Upsilon$ such that the cost function (3.10) is minimized subject to the state inequality constraints (3.11) and the terminal state constraints (3.12).

For each p, Problem $\hat{\text{P}}$ can be solved as a nonlinear optimization problem where the cost function (3.10) is minimized subject to the state constraints (3.11) and (3.12). Existing gradient-based optimization methods can be used to solve Problem $\hat{\text{P}}$. For this, we need the gradient formulas of the cost function and the constraint functions. The gradient formulas of the cost function (3.10) and the state constraints (3.11) and (3.12) are given bellow.

Theorem 3.2. *The gradients of the cost function $\hat{J}$ with respect to $\boldsymbol{\sigma}$ and $\boldsymbol{\gamma}$ are given by*

$$\frac{\partial \hat{J}}{\partial \boldsymbol{\sigma}} = \int_0^1 \frac{\partial H_0(s, \hat{\boldsymbol{x}}(s), \boldsymbol{\sigma}, \boldsymbol{\gamma}, \boldsymbol{\lambda}_0(s))}{\partial \boldsymbol{\sigma}} \mathrm{d}s \quad (3.13)$$

and

$$\frac{\partial \hat{J}}{\partial \boldsymbol{\gamma}} = \int_0^1 \frac{\partial H_0(s, \hat{\boldsymbol{x}}(s), \boldsymbol{\sigma}, \boldsymbol{\gamma}, \boldsymbol{\lambda}_0(s))}{\partial \boldsymbol{\gamma}} \mathrm{d}s \quad (3.14)$$

where $H_0(s, \hat{\boldsymbol{x}}(s), \boldsymbol{\sigma}, \boldsymbol{\gamma}, \boldsymbol{\lambda}_0(s))$ is the Hamiltonian function for the cost function (3.10) given by

$$H_0(s, \hat{\boldsymbol{x}}(s), \boldsymbol{\sigma}, \boldsymbol{\gamma}, \boldsymbol{\lambda}_0(s)) = \boldsymbol{\lambda}_0(s)^{\mathrm{T}} \vartheta^p(s) \boldsymbol{f}(\boldsymbol{x}(t(s)), \boldsymbol{\sigma}, s)$$

and $\boldsymbol{\lambda}_0(s)$ is the solution of the co-state differential equation

$$\dot{\boldsymbol{\lambda}}_0(s)^{\mathrm{T}} = -\frac{\partial H_0(s, \hat{\boldsymbol{x}}(s), \boldsymbol{\sigma}, \boldsymbol{\gamma}, \boldsymbol{\lambda}_0(s))}{\partial \hat{\boldsymbol{x}}}, \ s \in [0,1]$$

with the boundary condition

$$\boldsymbol{\lambda}_0(1)^{\mathrm{T}} = \frac{\partial[-\hat{m}(1)]}{\partial \hat{\boldsymbol{x}}(1)}$$

Similarly, for the state constraints we have the following theorem.

Theorem 3.3. *For each $i = 1, \ldots, 10$, the gradients of the state constraints function $\hat{\boldsymbol{g}}$ with respect to $\boldsymbol{\sigma}$ and $\boldsymbol{\gamma}$ are given by*

$$\frac{\partial \hat{g}_i}{\partial \boldsymbol{\sigma}} = \int_0^1 \frac{\partial H_i\left(s, \hat{\boldsymbol{x}}\left(s\right), \boldsymbol{\sigma}, \boldsymbol{\gamma}, \boldsymbol{\lambda}_i\left(s\right)\right)}{\partial \boldsymbol{\sigma}} \mathrm{d}s \tag{3.15}$$

and

$$\frac{\partial \hat{g}_i}{\partial \boldsymbol{\gamma}} = \int_0^1 \frac{\partial H_i\left(s, \hat{\boldsymbol{x}}\left(s\right), \boldsymbol{\sigma}, \boldsymbol{\gamma}, \boldsymbol{\lambda}_i\left(s\right)\right)}{\partial \boldsymbol{\gamma}} \mathrm{d}s \tag{3.16}$$

where $H_i\left(s, \hat{\boldsymbol{x}}\left(s\right), \boldsymbol{\sigma}, \boldsymbol{\gamma}, \boldsymbol{\lambda}_i\left(s\right)\right)$ is the Hamiltonian function for the state constraints function (3.11) and (3.12) given by

$$H_i\left(s, \hat{\boldsymbol{x}}\left(s\right), \boldsymbol{\sigma}, \boldsymbol{\gamma}, \boldsymbol{\lambda}_i\left(s\right)\right) = \boldsymbol{\lambda}_i\left(s\right)^{\mathrm{T}} \vartheta^p\left(s\right) \boldsymbol{f}\left(\boldsymbol{x}\left(t\left(s\right)\right), \boldsymbol{\sigma}, s\right)$$

and $\boldsymbol{\lambda}_i\left(s\right)$ is the solution of the co-state differential equation

$$\dot{\boldsymbol{\lambda}}_i\left(s\right)^{\mathrm{T}} = -\frac{\partial H_i\left(s, \hat{\boldsymbol{x}}\left(s\right), \boldsymbol{\sigma}, \boldsymbol{\gamma}, \boldsymbol{\lambda}_i\left(s\right)\right)}{\partial \hat{\boldsymbol{x}}}, \ s \in [0, 1]$$

with the boundary condition

$$\boldsymbol{\lambda}_i\left(1\right)^{\mathrm{T}} = \frac{\partial \hat{\boldsymbol{g}}\left[\hat{\boldsymbol{x}}\left(1\right)\right]}{\partial \hat{\boldsymbol{x}}\left(1\right)}$$

At this stage, we see that Problem P is approximated by a sequence of optimal parameter selection problems Problem $\hat{\mathrm{P}}$, each of which can be viewed as a mathematical programming problem and hence can be solved by existing gradient-based optimization methods. The optimal control software MISER 3.3 [9] was implemented based on these ideas, where the control is approximated by piecewise constant functions (i.e., in terms of zero order spline basis functions) or piecewise linear functions (i.e., in terms of first order spline basis functions). It is used here to solve our minimum-fuel low-thrust non-coplanar orbit transfer problem. Intuitively, the larger the p, the closer Problem $\hat{\mathrm{P}}$ is to Problem P.

4 Numerical Simulations

To illustrate the theory more explicitly, consider that a spacecraft with initial mass $m_0 =$ 500kg is propelled with constant thrust $T = \frac{1}{20} m_0 g_0$, where g_0 is the gravitational acceleration on the Earth surface and the specific impulse $i_{sp} = 600$s. By referring to the coordinate system defined in Figure 1, the initial conditions, $r_0 = 2$ DU, $\theta_0 = 0^\circ$, $\phi_0 = 0^\circ$, $u_0 = 0$ DU/TU, $v_0 = \sqrt{\frac{\mu}{r_0}}$, $w_0 = 0$ DU/TU, where DU and TU are the canonical distance and time unit [2], respectively. Here 1 DU is defined as the length of the radius of the Earth's equator and 1 DU/TU is defined as the circular orbit speed with the radius of 1 DU. From both definitions, the time units 1 TU can be derived. The final conditions, the radius of circular target orbit set to 5 DU, the inclination angle $i = 20^\circ$ and the longitude of the ascending node $\Omega = -120^\circ$.

The scaled time interval is $s \in [0, 1]$, which is partitioned into 20 equal subintervals. Terminal time of the orbit transfer is free to vary. For comparison, we have also solved the optimal control problem, which the cost function (2.13), system (2.18), the state inequality constraints (2.21) and the terminal state constraints (2.22), by both the proposed parametrization method (PM) and the second-order gradient method (SOGM) [4]. By using the SOGM and the PM, it is possible to obtain the optimal transfer trajectories as shown

in Figure 4-9. In these figures, the trajectories (computed by using the second-order gradient method, SOGM) are represented with the 'solid' lines, while the transfer trajectories computed by the proposed parametrization method (PM) are represented with the 'dashed' lines.

Figure 4 shows the three-dimensional optimal transfer trajectories. The two thinner lines represent both the original circular orbit (inner circle) and the circular target orbit. From the figure, it is found that the transfer trajectory computed by using the PM is very close to the optimal transfer trajectory obtained by using the SOGM.

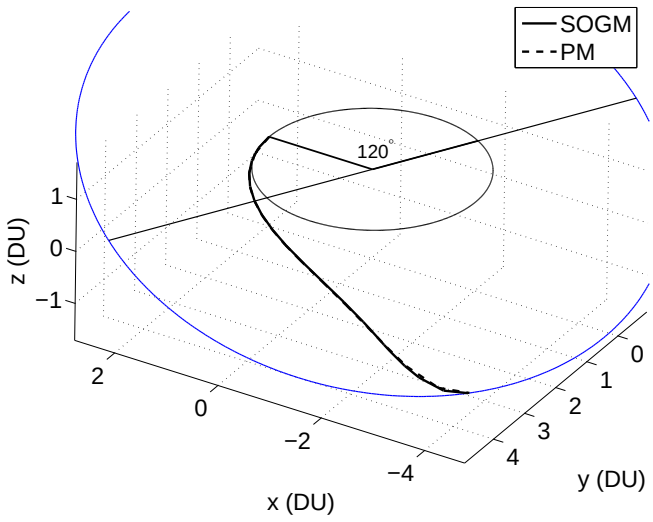

Figure 4: Comparison of the minimum-fuel trajectories computed by using the PM and the SOGM

Figure 5 shows the relationship between the radial distances r and the time t, computed by using the PM and SOGM. From the radial distances plotted in this figure, it is found that, with the result obtained by using the SOGM as standard, the result obtained by using the PM can characterize the optimal trajectory. The final radial distance $r(t_f)$ all satisfies the terminal constraint 5 DU. Figure 6 shows the relationship between the out-of-plane angle ϕ and the time t. It is found that, the out-of-plane angles are negative all the time. The reason is that the shortest ways to reach the target orbit are on the negative side of z coordinate, as can be seen from the geometric relationship between the original and the target orbit in Figure 4. From the figure, the errors of the results obtained by using the PM are almost negligible as compared with those obtained by using the SOGM. Figure 7 shows the relationship between the radial speed u and the time t. Obviously, from this figure it is found that the radial speeds vanish at the terminal time. The radial speeds increase near linearly to reach some maximum value and then decrease also near linearly. The maximum radial speed obtained by using the SOGM is larger than the one obtained by using the PM. Figure 8 shows the relationship between the circumferential speed v and the time t. The velocity component $v(t)$ increases to some maximum value shortly after the beginning, decreases thereafter to some minimum value and then increases again in short time to satisfy the terminal condition. The minimum circumferential speed obtained by using the SOGM

is smaller than the one obtained by using the PM. It is observed that all the curves have the similar pattern. Figure 9 shows the relationship between the out-of-plane speed w ant the time t. It is found that, the out-of-plane speeds are negative all the time. It decreases for a long period to some minimum value which is even smaller than the required value, and then it finally increases to reach terminal constraint.

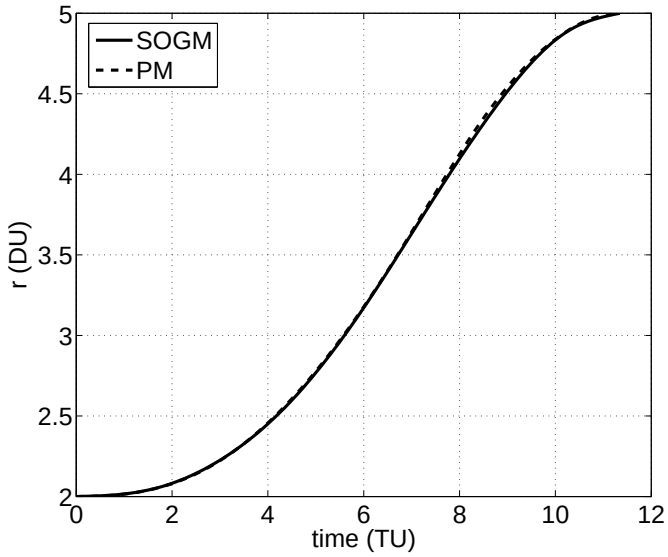

Figure 5: Comparison of the radial distances computed by using the PM and the SOGM

Figure 10 and 11 depict the optimal in-plane and out-of-plane thrust control angles φ and the time t, respectively. From the two figures, it is found that the optimal thrust control angles computed by using the PM and the SOGM have the same pattern, also satisfying the control constraints (2.21).

To further understand the accuracy of the proposed parametrization method, terminal conditions of the minimum-fuel low-thrust non-coplanar orbit transfer obtained by using the PM and the SOGM are listed in Table 1.

Table 1: Comparison of the terminal conditions computed by using the PM and the SOGM

Method	t_f(TU)	$\theta(t_f)(^\circ)$	$\phi(t_f)(^\circ)$	$v(t_f)(\frac{\mathrm{DU}}{\mathrm{TU}})$	$w(t_f)(\frac{\mathrm{DU}}{\mathrm{TU}})$	$m(t_f)$(kg)
SOGM	11.3447	140.7527	−19.7637	0.4473	−0.0246	118.6250
PM	11.3664	141.3149	−19.7888	0.4466	−0.0231	117.9300

From the Table 1, it is observed that as compared with the fuel consumptions obtained by using the SOGM, those obtained by using our method are only 0.14% more. The principal result here is that only a few parameters are required to approximate the optimal transfer trajectory well. This largely reduces the complexity of the control function as compared to that generated by the SOGM.

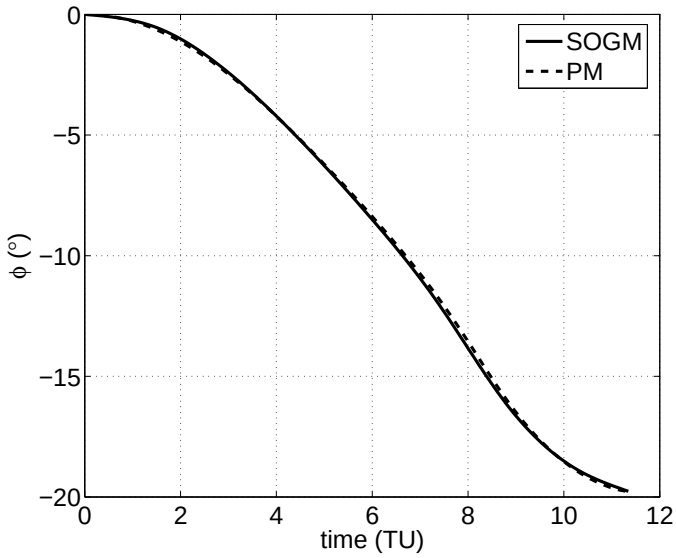

Figure 6: Comparison of the out-of-plane angles computed by using the PM and the SOGM

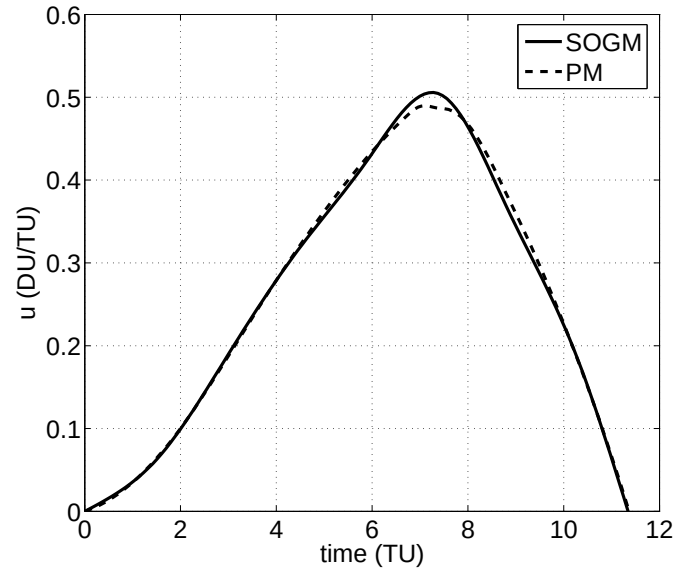

Figure 7: Comparison of the radial speeds computed by using the PM and the SOGM

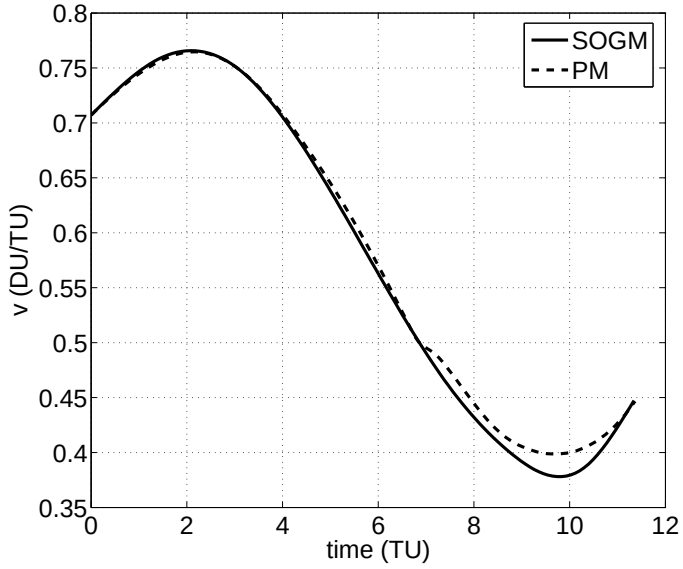

Figure 8: Comparison of the circumferential speeds computed by using the PM and the SOGM

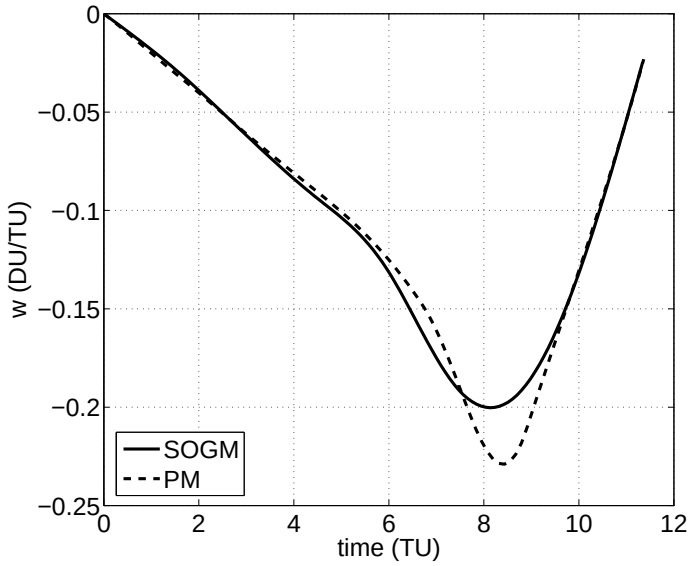

Figure 9: Comparison of the out-of-plane speeds computed by using the PM and the SOGM

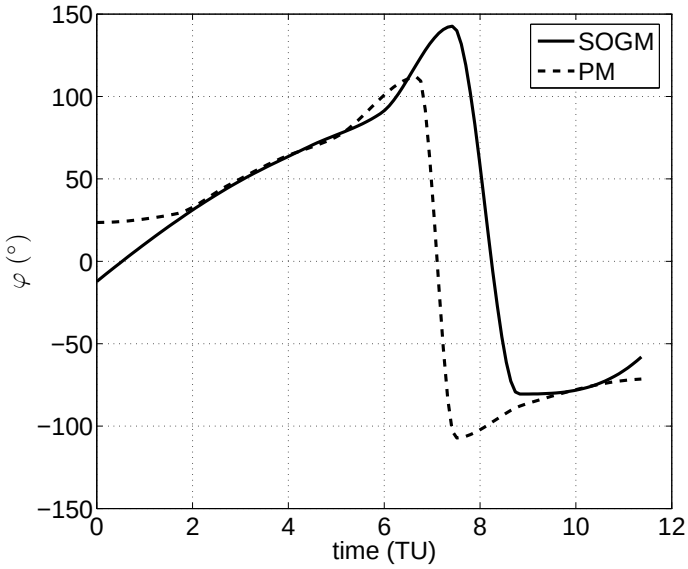

Figure 10: Comparison of the in-plane thrust control variables computed by using the PM and the SOGM

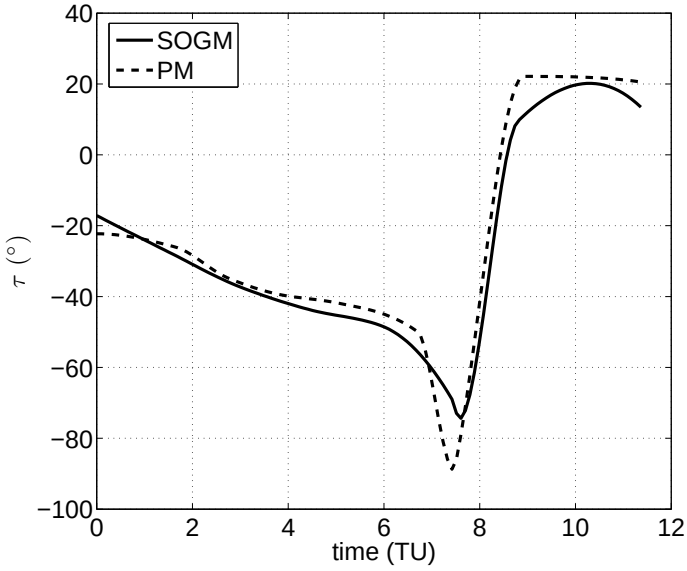

Figure 11: Comparison of the out-of-plane thrust control variables computed by using the PM and the SOGM

5 Conclusion

It is well-known that spacecraft is required to make some orbit transfers which are very fuel consuming. Moreover, after launched, the fuel of the spacecraft can not be replenished in the space, thus the minimum-fuel low-thrust non-coplanar orbit transfer mission have been considered in this paper. The spherical coordinate system is used to describe the dynamics of the spacecraft, and the terminal constraints are derived.

By using the control parametrization technique and the time scaling transform, the optimal orbit transfer problem is approximated as an optimal parameter selection problem which has a finite number of decision variables. Then, the optimal control software package MISER 3.3, which is a gradient-based method, is utilized to solve such a parameter selection problem, and an optimal control law is thus obtained. Simulation results demonstrate that the proposed approach is highly effective.

References

[1] S. Alfano and J.D. Thorne, Circle-to-circle constant-thrust orbit raising, *J. Astronaut. Sci.* 42 (1994) 35–45.

[2] R.R. Bate, D.D. Mueller and J.E. White, *Fundamentals of Astrodynamics*, Dover, New York, 1971.

[3] J.T. Betts, Optimal interplanetary orbit transfers by direct transcription, *J. Astronaut. Sci.* 42 (1994) 247–268.

[4] A.E. Bryson and Y.C. Ho, *Applied Optimal Cotrol Optimization, Estimation, and Control*, Taylor & Francis Group, New York, 1975.

[5] Y.M. Chen and D.L. Sheu, Parametric optimization analysis for minimum-fuel low-thrust coplanar orbit transfer, *J. Guid. Control. Dynam.* 29 (2006) 1446–1450.

[6] A.L. Herman and B.A. Conway, Direct optimization using collocation based on high-order Gauss-Lobatto quadrature rules, *J. Guid. Control. Dynam.* 19 (1996) 592–599.

[7] A.L. Herman and B.A. Conway, Optimal, low-thrust, Earth-Moon orbit transfer, *J. Guid. Control. Dynam.* 21 (1998) 141–147.

[8] A.L. Herman and D.B. Spencer, Optimal, low-thrust earth-orbit transfers using higher-order collocation methods, *J. Guid. Control. Dynam.* 25 (2002) 40–47.

[9] L.S. Jennings, M.E. Fisher, K. L. Teo and C.J. Goh, Miser3, Optimal control software version 3: theory and user manual, Centre for Applied Dynamics and Optimization, The University of Western Australia, URL: http://www.cado.uwa.edu.au/miser/manual.html, 2004.

[10] C.A. Kluever, Optimal low-thrust interplanetary trajectories by direct method techniques, *J. Astronaut. Sci.* 45 (1997) 247–262.

[11] C.A. Kluever and B.L. Pierson, Optimal low-thrust three-dimensional Earth-Moon trajectory, *J. Guid. Control. Dynam.* 18 (1995) 830–837.

[12] R. Loxton, K.L. Teo, V. Rehbock and K.F.C. Yiu, Optimal control problems with a continuous inequality constraints on the state and control, *Automatica J. IFAC* 45 (2009) 2250–2257.

[13] W.A. Scheel and B. A. Conway, Optimization of very-low-thrust, many-revolution spacecraft trajectories, *J. Guid. Control. Dynam.* 17 (1994) 1185–1192.

[14] S. Tang and B.A. Conway, Optimization of low-thrust interplanetary trajectories using collocation and nonlinear programming, *J. Guid. Control. Dynam.* 18 (1995) 599–604.

[15] J.D. Thorne and C.D. Hall, Minimum-time continuous-thrust orbit tansfers, *J. Astronaut. Sci.* 45 (1997) 411–432.

[16] L.Y. Wang, W.H. Gui, K.L. Teo, R. Loxton and C. Yang, Time delayed optimal control problems with multiple characteristic time points: computation and industrial applications, *J. Ind. Manag. Optim.* 5 (2009) 705–718.

[17] C.Z. Wu and K.L. Teo, Global impulsive optimal control computation, *J. Ind. Manag. Optim.* 2 (2006) 435–450.

Manuscript received 10 February 2012
revised 2 June 2012, 4 September 2012
accepted for publication 17 September 2012

Da-Ke Gu
School of Automation and Engineering, Northeast Dianli University, Jilin 132012, P.R. China
E-mail address: dakegu@gmail.com

Ling-Fang Sun
School of Automation and Engineering, Northeast Dianli University, Jilin 132012, P.R. China
E-mail address: sunlf@mail.nedu.edu.cn